



# Evaluation of *Artocarpus heterophyllus* seed performance and kinetics in the coagulation–flocculation process for the purification of paint industrial wastewater

Ifeoma MaryJane Iloamaeke<sup>1</sup> · Kelvin Obazie<sup>1</sup> · Mmesoma Offornze<sup>1</sup> · Chiamaka Marysilvia Ifeaghalu<sup>1</sup> · Cecilia Aduaka<sup>1</sup> · Ugomma Chibuzo Onyeije<sup>1</sup> · Claudine Ifunanaya Ogu<sup>1</sup> · Ngozi Anastasia Okonkwo<sup>1</sup> · Nnaemeka Nnaji<sup>2,3</sup>

Received: 17 February 2023 / Accepted: 2 July 2024 / Published online: 11 July 2024  
© The Author(s) 2024

## Abstract

The *Artocarpus heterophyllus* (AH) seed was used as a coagulant in this study to explore the effects of pH, settling time, and coagulant doses on the removal of colour, turbidity, and heavy metals from paint industrial wastewater. The AH coagulant was instrumentally characterized by SEM, FTIR, and XRD. The maximum colour and turbidity removal efficiencies were 94.33% and 99.94% at the dosage of 0.2 g/L, pH 2. The mercury removal efficiency of 99.29% was achieved at the optimal conditions of 0.8 g/L coagulant dosage and pH 8. At a dose of 1.0 g/L and a pH of 10, the highest lead removal efficiency was 99.76%. The best removal efficiency for arsenic was 75.24% at a 0.8 g/L coagulant dosage and pH of 8. All at a time of 50 and 40 min, respectively. XRD diffraction results before treatment depict that the AH coagulant was crystalline and changed to amorphous after treatment. The SEM and FTIR results of the coagulant revealed changes in the surface morphology and functional groups before and after treatment. The reaction kinetics were best modelled in second order.

**Keywords** *Artocarpus heterophyllus* · Coagulant · Treatment · Paint effluent · Heavy metals

## Introduction

Nigeria is a developing country with a population of more than 120 million people. Manufacturing industries are one of the activities that drive the economy. These industries, both small-, medium-, and large-scale manufacturers, are scattered throughout Nigeria's state. Unfortunately, the wastewater generated therefrom has seriously threatened the environment and aquatic lives. The pollutants, therefore, constitute a major concern and strain on water bodies as most of their discharge plants are channelled towards

rivers, lakes, streams, etc., without adequate treatment. In some regions, surface water is the community's only source of water, exposing them to health risks. According to statistics, by 2050, over two-thirds of the world's population will have inadequate access to good and clean potable water (Liu et al. 2018). This can be seen in the rise of contemporary industries and advanced farming practices, which produce a slew of toxins daily, poisoning water bodies at frightening levels. The demand for clean and potable water is increasingly becoming a topic of concern domestically and globally, as evidence of increased contamination of water bodies from anthropogenic and geological activities emerges (Pena et al. 2005). As a result, wastewater treatment and reuse are critical methods for fulfilling the growing demand for potable water. The proliferation of small-scale paint industries is an alarming increase because of the rate of unemployment and most of them are struggling to survive. Hence, need for a cost-effective coagulant and a method of treatment that is simple to use. Paint industrial effluent is alkaline, turbid, high in BOD, COD, heavy metals, suspended solids, coloured, etc. (Mohsen et al. 2010; Malakootian et al.

✉ Ifeoma MaryJane Iloamaeke  
im.iloamaeke@unizik.edu.ng; ifeomailoamaeke@yahoo.com

<sup>1</sup> Department of Pure and Industrial Chemistry, Nnamdi Azikiwe University, Awka, Anambra, Nigeria

<sup>2</sup> Department of Chemistry, Alex Ekwueme Federal University, Ndufu-Alike, Ikwo, Ebonyi State, Nigeria

<sup>3</sup> Department of Chemical and Minerals Engineering, North–West University, Potchefstroom, North West 2531, South Africa

2008; Abdoulhassan et al. 2016). The pigments, solvents, additives, and binders added to the paint during production are responsible for the heavy metals, colour, and turbidity of the paint industry wastewater (Vishali, and Agrawal 2017). The colours used to make paint are called pigments. Iron oxides, titanium dioxide, lead chromates, cadmium, chromium oxide, and mixed metal oxides are a few examples. The kind of paint determines the type of solvent. While oil-based paint uses organic solvents like toluene, benzene, mixed xylene, etc., latex paint uses water. Emulsifiers, deformers, thickening and anti-setting agents, wetting and dispersion agents, biocides, etc., are examples of additives. Synthetic or natural resins, such as acrylics, polyurethanes, polyesters, melamine resins, epoxy, oils, etc., are examples of binder materials.

Colour is an organic material that has dissolved into a solution, while turbidity consists of tiny particles suspended in the water column (Hubbe et al. 2016). Coloured water has negative consequences for aquatic ecosystems by hindering the photosynthetic process of water organisms (Elango and Elango 2017), including water's aesthetic appeal (Ahmadi and Zanjanchi 2016) and rendering the water unfit for consumption and domestic purposes (Ghernaout et al. 2015).

Raychaudhuri et al. (2021) and Yadav et al. (2020) defined heavy metals as metals and metalloids with an atomic number greater than 20 and an atomic density greater than  $5 \text{ g/cm}^3$  that are toxic even at low parts per billion (ppb) concentrations. They are non-biodegradable, have a proclivity for accumulating in living things, and may cause cancer. Long-term and continuous exposure to heavy metals has been linked to several health risks (Yadav et al. 2020). Lead is dangerous to one's health and can impair the kidneys, liver, reproductive system, and brain (Naseem and Tahir 2001). Mercury is a neurotoxin that has the potential to harm the central nervous system. If the concentration is too high, it might cause pulmonary discomfort, chest discomfort, and dyspnoea (Namasivayam and Kadirvelu 1999). Arsenic may lead to cancer of the skin, lungs, bladder, and kidneys malfunctioning, as well as muscle weakness, appetite loss, and nausea (Mohan and Pittman 2007). As a result, these microscopic particles should be eliminated from industrial wastewater. Some cost-effective wastewater treatment technologies include catalytic ozonation, mesoporous membrane, ultrafiltration, and microscreen (Ghuge and Saroha 2018; Al-Shehri et al. 2019; Niam et al. 2021; Lasaki et al. 2023a). The coagulation–flocculation process is mostly used as a process of treating water/wastewater because it is affordable and simple to use and many small-scale paint industries can adopt it as their treatment method (Gaikwad and Munavalli 2019; Jabar et al. 2020; Iloamaeke et al. 2021). Coagulation causes colloidal particles and suspensions to have a reduced electrokinetic potential, which permits them to aggregate (Jachimowicz and Cydzik-Kwiatkowska 2022).

Alum, ferric chloride, calcium hydroxide, sodium aluminate, aluminium chloride, and ferric sulphate are inorganic salts mostly used as coagulants. The issues found with these salts include (1) their potential to cause cancer and Alzheimer's disease (Okuda et al. 1999; Okolo et al. 2015); (2) their strong hydrolysis properties of  $\text{Fe}^{3+}$  limiting the polymerization of iron-based coagulants (Chen et al. 2015); (3) their low coagulation efficiency in cold water (Mohammed et al. 2012); (4) their non-biodegradability; and (5) their high sludge generation (Ani et al. 2011). Organic coagulants are cheap, renewable, biodegradable, and environmentally benign. Hence, the conceived use of AH seed as a coagulant. AH seed as a coagulant is a biomass from agriculture. The edible part of the AH fruit is eaten while the seeds are thrown away. This research, however, finds an application to this seed which is an innovation that converts waste products into wealth due to its efficacy in treating paint industrial wastewater. Recent studies on the use of agro-waste as coagulants by the coagulation–flocculation process are Kernel of *Moringa oleifera* and *Strychnos potatorum* (Nirmali) seeds, (Gaikwad and Munavalli 2019), *Treculia Africans* seed coat (Iloamaeke et al. 2020), *Moringa oleifera* seed coat (Jabar et al. 2020), *Mercenaria mercenaria* shell (Iloamaeke et al. 2021). Research on the use of *Artocarpus heterophyllus* (Jackfruit) seed as a coagulant has shown that Jackfruit seed extract in NaCl has been used to remove turbidity and coliform bacteria from drinking water (Natumanya and Okot-Okumu 2015). Anu and Anu (2016) recorded the usage of Jackfruit seed powder to remove turbidity, conductivity, and total suspended matter from dairy wastewater collected from the industry. Also, Suffian Yusoff et al. (2016) investigated the effect of Jackfruit seed starch as a coagulant aid in the poly aluminium chloride coagulant for the removal of colour, COD, turbidity, suspended solids, and ammoniacal nitrogen from landfill leachate.

None of these studies demonstrated the use of the AH seed in the removal of colour, turbidity, and heavy metals from the paint industry effluent, the functional groups responsible for the removal of the pollutants, the surface morphology of the coagulant, the crystallinity of the coagulant (AH), and the coagulation–flocculation kinetics. It is the aforementioned gap that this study tends to fill.

The study is aimed at investigating the performance potential of (AH) seed as a coagulant in the removal of colour, turbidity, and heavy metals such as lead, arsenic, and mercury from paint industrial wastewater. Physico-chemical analysis of paint wastewater was determined including characterization of the AH coagulant before and after coagulation–flocculation. The kinetics performance of the process was equally elucidated.

## Materials and methods

### Collection of paint effluent sample

A grab sampling technique was employed. The paint industry wastewater was collected from the waste channel pipe of Evangel Paint and Chemicals, located at Eke-Awka, Awka South Local Government, Anambra State of Nigeria. The colour of this effluent was milk. The effluent was collected in 10 L of a black gallon, tightly closed, and stored in a cool place at 4 °C. The characteristics of the paint effluent are presented in Table 1.

### Preparation of AH Coagulant

The AH fruit was purchased at Eke-Awka market in Awka, Anambra State. The edible body was eaten, leaving the seed (Fig. 1), which was sun-dried for two weeks to remove moisture, after which it was ground using a grinder until its particles were reduced to a powder of a particle size of 1.18 µm using a sieve, thereafter it was kept in a dry container.

### Physicochemical analysis

Chemical oxygen demand (COD), biological oxygen demand (BOD), total dissolved solids (TDS), total suspended solids (TSS), total hardness, chloride, phosphate, nitrate, and sulphate concentrations were all measured. They were carried out following the standard method for water and waste analysis as stated in Table 1 (procedure in the supplementary material). The electrical conductivity, turbidity, and pH of the paint wastewater were all measured using an electrical conductivity metre (DDS-307 New Delhi, India),



Fig. 1 The seed of *Artocarpus heterophyllus*

turbidimeter (Lab. Tech. model 038, India), and a pH metre (Hanna model HI991300 USA), respectively. Heavy metals were analysed with an atomic absorption spectrophotometer (AAS) (Agilent technology, USA) according to the APHA 3112B (2012) method. Proximate analysis was done using a standard procedure (AOAC 1990a; 2000a; 2000b; 2005b). The characteristic of the paint effluent collected is shown in Table 1.

### Instrumental characterization of the AH coagulant

Functional groups, crystallinity, and the surface morphology of AH coagulant were characterized using standard methods and instruments such as FTIR spectrometer model Cary 630 Agilent tech., Inc USA), XRD spectrometer (Rigaku mono

**Table 1** Characteristics of paint industry wastewater

Parameters	Paint wastewater before treatment	Methods of determination	FEPA (1999)	WHO (2006)
Colour	Milk	–	–	–
pH	7.14 ± 0.08	APHA 4500-H (1992)	5–9	6.5–8.5
Temp. (°C)	30 ± 0.56	APHA 2550A (1992)	< 40	–
TDS (mg/L)	1400 ± 11.5	APHA 2540 C (1998)	2000	500
TSS (mg/L)	63.40 ± 0.46	APHA 2540 D (1998)	30	30
Turbidity (NTU)	360 ± 8.08	EPA 180.1 (1993)	–	5
Hardness (mg/L as CaCO <sub>3</sub> )	13.78 ± 0.32	APHA 2340-B (2012)	–	70
BOD (mg/L)	63.00 ± 0.31	APHA 5210B (1992)	40	35
SO <sub>4</sub> <sup>2-</sup> (mg/L)	1.16 ± 0.012	APHA 2510-B (1998)	500	250
COD (mg/L)	121.70 ± 0.17	APHA 5220 D (1998)	80	–
PO <sub>4</sub> <sup>3-</sup> (mg/L)	16.40 ± 0.67	APHA 5220 D (1998)	5	–
Mercury (mg/L)	1.392 ± 0.083	APHA 3112B (1995)	0.05	0.001
Lead (mg/L)	0.254 ± 0.010	APHA 3112B (1995)	0.01	0.01
Arsenic (mg/L)	1.236 ± 0.064	APHA 3112B (1995)	0.1	0.01

flex 600 by Rigaku cooperation, Japan), and SEM (model Phenom-ProX, Netherlands), respectively.

### Coagulation–flocculation experiment

The Jar test method was employed in this experiment. Exactly 0.2 g of AH coagulant was weighed into a 250-mL beaker containing 100 mL of paint wastewater made to be at pH 2. The pH is adjusted by adding 1.0 M HCl for acidic pH or 1.0 M NaOH for basic pH to the paint wastewater. The content of the beaker was stirred for 2 min of rapid mixing (100 rpm) and 20 min of slow mixing (40 rpm) with a magnetic stirrer and then left undisturbed for 50 min. It was filtered (0.5  $\mu\text{m}$  Whatman No. 1 filter paper) and the filtrate was subjected to turbidity, colour, and heavy metal removal analysis using a turbidimeter (Lab. Tech. model 038, India), UV/VIS spectrophotometer (Apel 3000uv, Japan) at 340 nm  $\lambda$  max and an atomic absorption spectrophotometer (Agilent tech. USA), respectively. The experiment was repeated for the dosages of 0.4, 0.6, 0.8, and 1.0 g/L and pH 4, 6, 8, and 10 at a constant 50 min settling time. For the effect of time on the removal efficiency, pH 2 was kept constant and the settling time varied from 10, 20, 30, 40, and 50 min, while for heavy metals pH of 10 and 8 were constant and the same ranges of time varied against coagulant dosages. The experiments were monitored for the effect of coagulant dosage (AH), pH and time on the colour, turbidity, mercury, lead, and arsenic removal efficiency (% I). The colour, turbidity, and heavy metals removal efficiency were calculated thus:

$$\% I = \frac{\text{initial concentration} - \text{final concentration}}{\text{initial concentration}} \times 100 \quad (1.1)$$

The data collected from the coagulation–flocculation experiment were used for the kinetics study aspect of this work.

### Coagulation–flocculation kinetics—theoretical considerations

According to Menkiti and Onukwuli (2011), the Brownian diffusion coefficient ( $D$ ) has the following expression, Eq. (1.2)

$$D = \frac{K_B T}{6\pi\eta_o r} \quad (1.2)$$

Abel et al. (1994) showed that the rate constant is a product of collision efficiency,  $\varepsilon$ , and the Smoluchowski rate constant of rapid coagulation,  $k_R$

$$k = \varepsilon k_R \quad (1.3)$$

The Smoluchowski rapid coagulation rate constant has this expression in the equation (Ani et al. (2010)

$$k_R = \frac{4K_B T}{3\eta_o} \quad (1.4)$$

where  $k_B$  represents the Boltzmann constant,  $T$  signifies absolute temperature, and  $\eta_o$  is the viscosity of the fluid. Equation 1.5 is obtained by combining Eqs. 1.3 and 1.4

$$k = \frac{4\varepsilon k_B T}{3\eta_o} \quad (1.5)$$

Brownian diffusion coefficient ( $D$ ) has the following expression (Nnaji et al. 2014)

$$D = \frac{K_B T}{6\pi\eta_o r} \quad (1.6)$$

Expression for effluent viscosity  $\eta_o$  is obtained by making  $\eta_o$  the subject of the formula in Eq. 1.6

$$\eta_o = K_B T / 6\pi D r \quad (1.7)$$

Substituting Eq. (1.7) in Eq. (1.4) and making collision efficiency,  $\varepsilon$  subject of the formula gives Eq. 1.8

$$\varepsilon = \frac{k}{8\pi D r} \quad (1.8)$$

Brownian diffusion coefficient ( $D$ ) also is related to the friction factor,  $\beta$  (Okolo et al. 2015).

$$D = \frac{K_B T}{\beta} \quad (1.9)$$

An expression for friction factor ( $\beta$ ) is obtained by substituting Eqs. (1.9) in Eq. (1.6)

$$\beta = 6\pi\eta_o r \quad (2.0)$$

Menkiti and Onukwuli, (2011) gave the following relationship between the friction factor,  $\beta$  and the coagulation–flocculation rate constant,  $k$

$$\beta = 2k \quad (2.1)$$

Effluent viscosity can also be obtained by substituting Eq. (2.1) in (2.0) which gives Eq. 2.2

$$\eta_o = \frac{k}{3\pi r} \quad (2.2)$$

where  $\eta_o$  is the effluent viscosity and  $r$  is the particle radius. In this study, it is obtained from sieve particle measurement.

First- and second-order equations are shown, respectively, in Eq. (2.3) and (2.4)

$$\ln N_t = \ln N_0 - kt \quad (2.3)$$

$$\frac{1}{N_t} = \frac{1}{N_0} + kt \tag{2.4}$$

Coagulation–flocculation period  $\tau_{1/2}$  is given as;

$$\tau_{1/2} = \frac{1}{0.5k[N]_0} \tag{2.5}$$

where  $N_t$  is the concentration of the coagulant dosage at the time  $t$ ,  $t$  is the settling time,  $N_0$  is the initial concentration of the particles, and  $k$  can be called the turbidity removal rate constant.

## Results and discussion

### Proximate composition of AH coagulant

The result of the proximate parameters of the AH coagulant obtained in this study is presented in Table 2. According to Mohamad et al. (2019), Sreeletha et al. (2017), and Suzihaque et al. (2022), carbohydrates and proteins are the major components of jackfruit seeds. The proximate analysis shows that the seed of AH contains the highest amount of protein and carbohydrate which is needed in this study as a precursor. Organic compounds contain carbon which plays a critical role in the adsorption and removal of metals, colours, and particles from wastewater because of their porous nature (Jatto et al. 2010). Carbohydrates and proteins are desirable in the adsorption and coagulation–flocculation process

**Table 2** Proximate composition of the *Artocarpus heterophyllus* coagulant

Parameters (%)	AH coagulant	Methods of determination
Moisture	8.82 ± 0.39	AACC method number: 44-15A
Ash	4.00 ± 0.80	AOAC method 942.05
Fat	3.56 ± 0.46	AOAC method 920.39
Protein	26.63 ± 0.53	AOAC method 945.18-B
Crude fibre	12.27 ± 0.27	AOAC method 978.10
Carbohydrate	43.72 ± 0.25	AOAC (differential method)

**Table 3** Comparison of the proximate composition of AH with other researchers

Parameters (%)	Current study	Suzihaque et al. 2022	Sivaranjini et al. 2020	Mohamad et al. 2019	Sultana et al. 2017	Fateatun et al. 2014	Sreeletha et al. (2017)
Moisture	8.82 ± 0.39	6.34	20.6	10.76	39.22	9.02	49.59
Ash	4.00 ± 0.80	3.74	2.43 +	2.4	1.30	2.66	-
Fat	3.56 ± 0.46	2.10	1.04	0.75	0.98	1.40	0.40
Protein	26.63 ± 0.53	11.83	7.77	13.67	16.01	11.34	13.6
Crude fibre	12.27 ± 0.27	-	1.3	3.00	3.56	-	-
Carbohydrate	43.72 ± 0.25	36.67	67.5	69.39	42.49	-	19.2

because they have –COOH and –NH<sub>2</sub> functional groups that aid this process (Menkiti et al. 2018; Asantewah et al. 2021). The result in Table 2 shows the moisture, ash, fat, protein, crude fibre, and carbohydrate contents of the AH seed as 8.82% ± 0.39, 4.00% ± 0.80, 3.56% ± 0.46, 26.63% ± 0.53, 12.27% ± 0.27, and 43.72% ± 0.25 sequentially. The comparison of this result with other researchers as presented in Table 3 shows that moisture contents (8.82%) and ash (4.00%) from our result compare well with the moisture content and ash content of Suzihaque et al. (2022) (6.34% and 3.74%), Fateatun et al. (2014) (9.02% and 2.66%), and Mohamad et al. (2019) (10.76 and 2.4%), respectively. There is an agreement between our fat content of 3.56% with that of 2.10% of Suzihaque et al. (2022), likewise, our carbohydrate content (43.72%) and that of Sultana et al. (2017) 42.49%. The disparity in the proximate analysis results can be attributed to the maturation of the seed, the geographical location of the growing plant including environmental factors.

### Effect of coagulant dosage, pH, and time on the removal efficiencies

Figure 2 depicts the plot of colour removal efficiency against pH for different coagulant dosages at a constant time of 50 min. The graphs show that the colour removal efficiency decreases as the coagulant dosage increases from 0.2 to 1.0 g/L. This is because, at 0.2 g/L the colloid particles of paint wastewater which is negatively charged destabilize, this results in charge neutralization, hence agglomerating into flocs which can easily be sedimented and filtered, thus a rise in the colour removal efficiency. Beyond 0.2 g/L of coagulant dosage, the colloid particles of the paint wastewater re-stabilize. In other words, charge reversal and coagulation recession occur. Increasing coagulant dosages will increase the positive charge of the coagulants, thus leading to electrostatic repulsion between particles (Islam and Mostafa 2020). Hence, results in a decline in the colour removal efficiency after optimal coagulant dosage are reached. The maximum colour removal efficiency is 94.33% at 0.2 g/L (Fig. 2a). The same observation is made in Fig. 2b

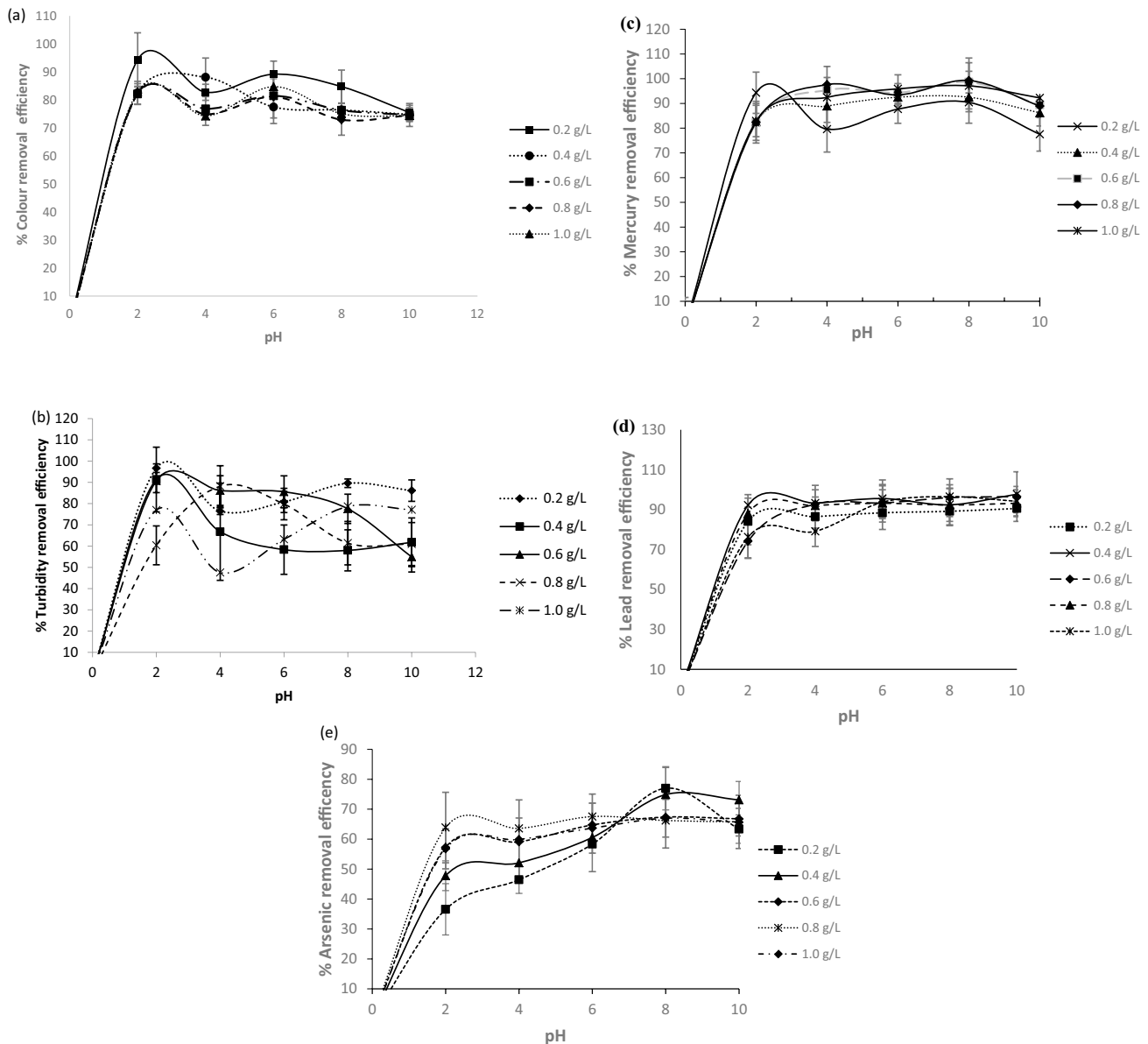


**Fig. 2** Plot of % removal efficiency against pH at different coagulant dosages at constant 50 min **a** colour removal **b** turbidity removal **c** mercury removal **d** lead removal **e** arsenic removal

and e, where the turbidity and arsenic removal efficiencies are 96.66%, and 77.01% at the peak of 0.2 g/L. This removal efficiency of turbidity 96.66% at the optimal dosage is comparable to the work of Lasaki et al. (2023b). While in Fig. 2c, and d, another trend of variation in the removal efficiency was observed. Figure 2c shows that mercury removal efficiency surges from 0.2 to 0.8 g/L and then decreases at 1.0 g/L. Figure 2d presents the lead removal efficiency rise from 0.2 to 0.4 g/L then witnesses a reduction from 0.6 to 1.0 g/L. The maximum mercury and lead removal efficiencies are 99.29% at 0.8 g/L and 97.72% at 0.4 g/L, respectively. The same re-stabilization of colloid particles after

optimal coagulant dosage is reached was predominant in the work of Menkiti et al. (2015a, b); Iloamae et al. (2021); Islam and Mostafa (2020).

The results in Figs. 2a–e demonstrated that the colour, turbidity, mercury, lead, and arsenic removal efficiencies were aided by the pH of the effluent. It is obvious in the results (Fig. 2a and b) that the colour and turbidity removal efficiencies dropped as the pH rose from 3 to 10. The best removal efficiency on both graphs 2a and 2b is pH 2. This is in agreement with the work of Mohanad et al. (2021) and Ngadi and Yusoff (2013). If the coagulation–flocculation condition is acidic, the density of positive charges on the

surfaces of the coagulant will be high; therefore, charge neutralization dominates the coagulation mechanism (Cao et al. 2010). While Fig. 2c, d, and e reports that the boost in removal efficiencies was brought about by the rise in pH from 2 to 10. Madukasi et al. (2009) suggested that this might be due to polar and hydrophilic functional groups in the effluent, which led to a faster aggregation at pH 2, 8, and 10, thus progression in the removal efficiency. The optimal removal efficiencies of mercury, arsenic, and lead were noted at pH 8 (Fig. 2c and e) and 10 (Fig. 2d), respectively. High pH means more alkaline and the coagulant surface will adopt a negative charge; thus, the adsorption mechanism overrides the removal of mercury, lead, and arsenic. A similar finding

has been documented by Sakhi et al. (2019), where the removal efficiency of the following heavy metals, such as Cd, Pb, Ni, Cr, As, and Se, was obtained at pH 8. Marzougui et al. (2018) and Pang et al. (2011) reported optimal pH of 8.5 for Pb, Cr, Zn, Cu, Ni removal and 8–10.9 for Pb, Zn, and Fe, respectively.

The effect of time on the coagulation–flocculation is plotted in Fig. 3a–e. This is the time for destabilization of the paint effluent's colloid particles and the floc's formation. Those graphs exhibit that time is another significant variable in treatment efficiency. As portrayed in the graphs, the best treatment performance was observed at 50 min and 0.2 g/L with colour (Fig. 3a), turbidity (Fig. 3b), lead (Fig. 3d), and

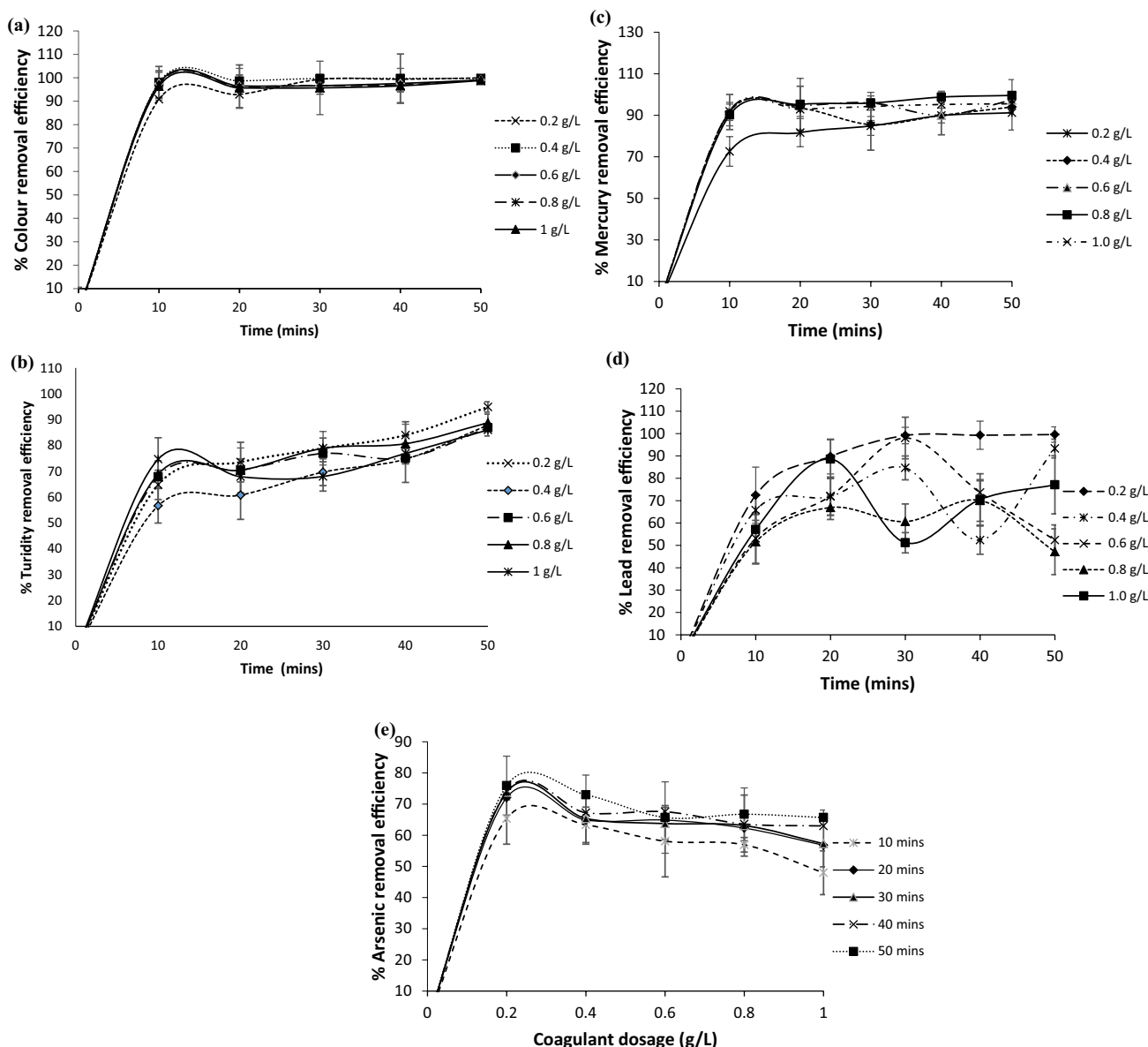


**Fig. 3** Plot of removal efficiency against time at different coagulant dosages **a** colour removal at constant pH 2 **b** turbidity removal at constant pH 2 **c** lead removal at constant pH 8 **d** mercury removal at constant pH 10 **e** arsenic removal at constant pH 8

arsenic (Fig. 3e) removal efficiencies of 94.90%, 99.94%, 99.56%, and 75.94%, respectively. Mercury (Fig. 3c) has the optimal treatment efficiency of 99.57% at 0.8 g/L at 40 min. This is because there were so many active coagulant sites accessible for destabilizing activities, and the coagulation rate was substantial at the beginning of the coagulation–flocculation process, as seen by the significant improvement in removal efficiencies achieved between 10 to 50 min (Menkiti et al. 2014; Abdulsahib et al. 2015). Lasaki et al. (2023a) reported that the settling time, which correlates with settling velocity, serves as an indicator for assessing the effectiveness of a flocculant in generating flocs that settle rapidly. Here, AH serves the dual function of a coagulant and flocculant. The settling time for this coagulation–flocculation process is between 40 and 50 min, indicating the duration required for the formation of highly settleable flocs and facilitating their easy removal through filtration, thereby enhancing pollutant removal efficiency. Additionally, the substantial size of the AH coagulant, as reported by Teh et al. (2014), might explain the rapid settling of the flocs formed. There is a concordance between these results and the results of the variation of coagulation dosage against pH with respect to coagulant dosage. This result is consistent with our earlier work (Iloamaeke and Julius 2019; Iloamaeke et al. 2021; Vajihinejad et al. 2019).

## IR analysis

The IR analysis was conducted before the treatment of the paint wastewater with the *Artocarpus heterophyllus* coagulant (AH) and the sludge (residue) after the treatment. The results are displayed in Fig. 4a–c, while the interpretation of the IR spectral bands is tabulated in Table 4. Table 4 can also be referred to as the functional groups' interaction of the colloid particles of the paint wastewater and the AH coagulants. From the Table, the following conclusion can be drawn about AH coagulant: the absorption peak at  $3655.5\text{ cm}^{-1}$  is assigned to O–H functional group from alcohol,  $3280.1$  and  $2822.2\text{ cm}^{-1}$  signify N–H stretch from amine and O–H stretch from carboxylic acid, confirming the presence of protein and carbohydrate in the proximate analysis (Table 2). Spectral bands at  $1952.5$  and  $1982.9\text{ cm}^{-1}$  are attributed to C–H bending,  $1636.3\text{ cm}^{-1}$  is N–H bending from amine,  $1405.2$  and  $1338.1\text{ cm}^{-1}$  are O–H bending from alcohol, while  $1148.0\text{ cm}^{-1}$  indicates C–O stretch from the ether. A similar result has been obtained by (Choy et al. 2016). Comparing the IR spectrum of AH coagulant (Fig. 4a) to the AH sludge of dosage and pH (Fig. 4b) and AH sludge of dosage and time (Fig. 4c) in the same Table 3, it can be observed that the peak at  $3655.5\text{ cm}^{-1}$  disappeared from the spectra of AH sludge of dosage and pH and AH sludge of dosage and time. A new absorption peak of  $1244.9\text{ cm}^{-1}$  and  $1237.5\text{ cm}^{-1}$  was added to the AH sludge of dosage and pH

including dosage and time, respectively. N–H bending was not in AH coagulant of dosage and time while other spectral bands were shifted upwards and downwards. This suggests that AH coagulant has removed pollutants from the paint wastewater. The functional groups that actively participate in the process are mostly amine, hydroxyl, and carboxylic groups, while the primary agents of the coagulation–flocculation process, according to Thamer and Eman (2017), are proteins.

## SEM analysis result of AH coagulant

The SEM result of the AH coagulant before the coagulation–flocculation process is delineated in Fig. 5a. A close observation of Fig. 5a reveals that the surface of this coagulant looks rough with tiny pores in it. The rough surface and pores are the points of attachment of the colloidal particles of the paint wastewater. This property makes the seed of AH a suitable precursor. Figure 5b is the surface morphology of the residue (sludge) after the coagulation–flocculation process of dosage and pH at a constant time of 50 min, while Fig. 5c is the surface morphology of the sludge of dosage and time at a constant pH. Figure 5b and c shows that the coagulant surfaces are compressed as a result of the rough porous nature of the coagulant surface which attracted the colloidal particles of the paint effluent and thus clumped together. These changes in the surface morphology of the coagulant after the coagulation–flocculation process demonstrated that AH coagulant removed pollutants from the paint wastewater.

## XRD result

X-ray diffraction (XRD) is an analytical technique for determining materials' crystallinity and amorphous nature. It functions by producing constructive interference with a crystalline sample and monochromatic X-rays (Menkiti and Ejimofor 2016). The AH coagulant (Fig. 6A) before treatment with paint wastewater exhibited five distinct peaks at  $28^\circ$ ,  $37^\circ$ ,  $43^\circ$ ,  $55^\circ$ , and  $58^\circ$  at 2 thetas, which are crisp, strong, and singularly extended up. This suggests strong crystallinity; however, the XRD patterns of the coagulant following treatment (Figs. B and C) exhibit wide, weak, and overlapping peaks, indicating poor crystallinity or amorphous structure. The overlapping peaks are due to the interaction of pollutants from paint industrial wastewater and the crystalline structure of AH coagulant.

## Coagulation–flocculation kinetics

The coagulation–flocculation reaction for a colloid particle of paint wastewater ( $P$ ) and AH coagulant ( $A$ ) is given as shown in Eq. 2.6



**Fig. 4** FTIR spectra of *Artocarpus heterophyllus* **a** coagulant before the coagulation–flocculation process **b** after the coagulation–flocculation process of dosage and pH **c** after the coagulation–flocculation process of dosage and time

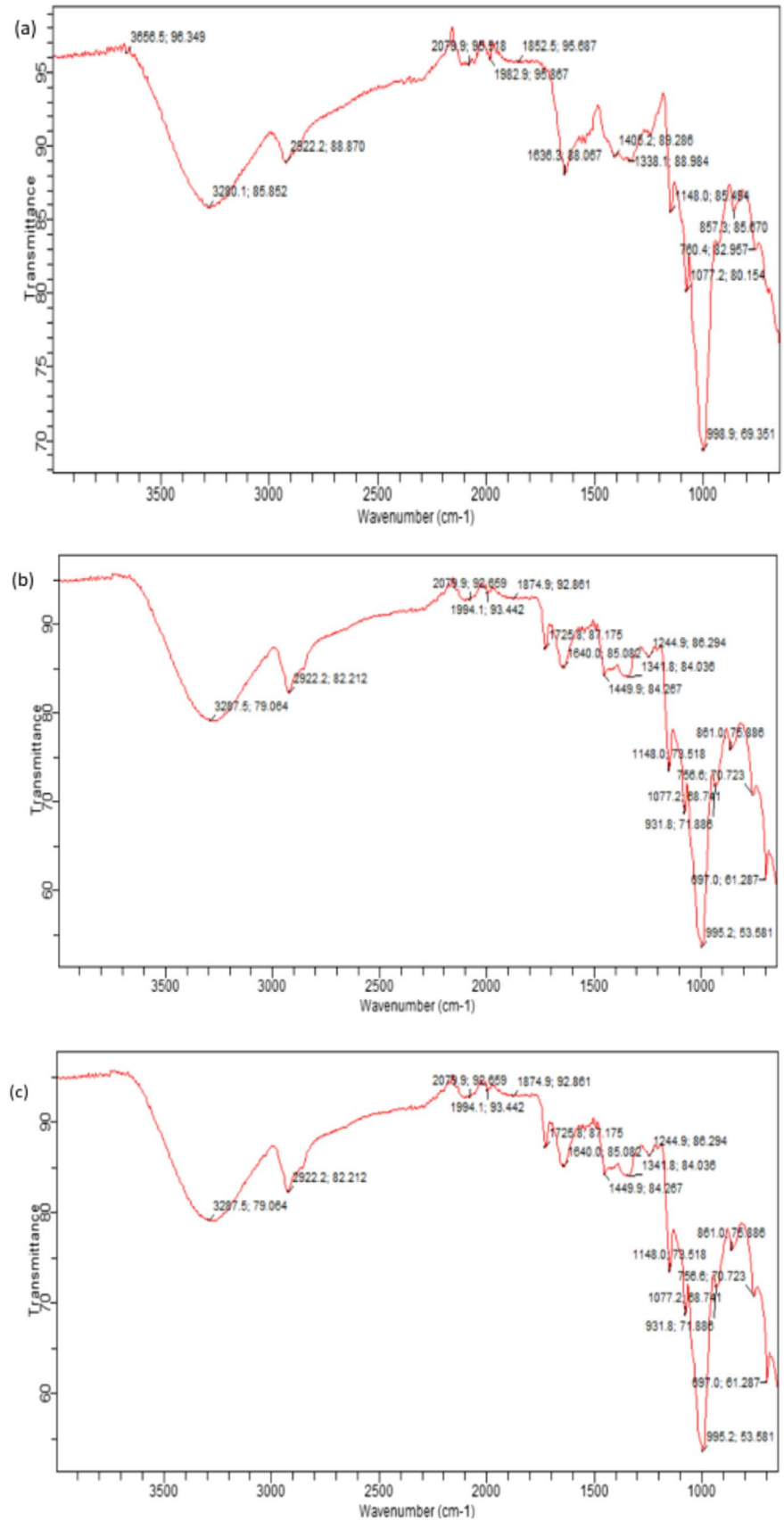
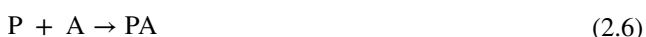


**Table 4** IR interpretation of spectral bands

AH coagulant spectral bands before treatment (cm <sup>-1</sup> )	AH sludge spectral bands (cm <sup>-1</sup> ) of dosage and pH	AH sludge spectral bands (cm <sup>-1</sup> ) of dosage and time	Assignment
3655.5	–	–	O–H stretch from alcohol
3280.1	3287.7	3283.8 and 3026.6	N–H stretch from the amine
2822.2	2922.2	2929.7 and 2870.1	OH stretch from carboxylic acid
1952.5 and 1982.9	1994.1, 1726.8	1990.4, 1871.1 1725.8, and 1654.9	C–H bend from aromatic compound
1636.3	1640.0	–	N–H bend from amine
1405.2 and 1338.1	1449.9 and 1341.8	1449.9 and 1356.8	O–H bending from alcohol
–	1244.9	1237.5	C–O stretch from alcohol
1148.0	1148.0 and 1077.2	1151.7, 1017.6, and 1103.3	C–O stretch from aliphatic ether



The rate equation of the above process is given as

$$r = k [p][A] \quad (2.7)$$

According to Eq. 2.7, the rate of these reactions depends on the  $k$  and concentration of both the colloid particles of paint wastewater and the AH coagulant. Figure 7 is the second-order reaction of the coagulation–flocculation process. Table 5 illustrates the functional coagulation–flocculation kinetics parameters for various dosages and times at constant pH 2 of the turbidity removal. The data of the turbidity removal at different coagulant dosages and time were used to study kinetics because it gave the highest treatment efficiency. The turbidity data were converted to milligrams per litre (mg/L) by multiplying turbidity in NTU by 2.2 (Menkiti et al. 2015a, b) and finally to grams per litre by dividing turbidity in mg/L by 1000.  $k$  is the coagulation–flocculation rate constant involved in the aggregation for the second-order predominated process. High  $k$  is also required to obtain low  $\tau_{1/2}$  since both are inversely proportional according to Eq. 2.8. The highest  $k$  is 0.0010 L/g min at 0.2 g/L.  $\epsilon$  is the particle collision efficiency which is directly proportional to the kinetic energy acquired by the colliding particles. The lowest  $\tau_{1/2}$  is obtained at 5.55556 min, which denotes the period for rapid coagulation–flocculation, resulting in particle aggregation and the formation of floc. High collision efficiency  $\epsilon$  leads to high kinetic energy required to overcome repulsive forces of attraction that hinder particles from aggregating and this is evident in Table 5. Furthermore, this explains why the highest turbidity efficiency is obtained at 0.2 g/L pH 2 and a time of 50 min. Other parameters such as  $k_R$  and  $\beta$  correlate well with the  $k$ ,  $\epsilon$  and  $\tau_{1/2}$ . This result agrees with the work reported elsewhere (Menkiti et al. 2015a, b; Ani et al. 2012; Vishali, and Karthikeyan 2018).

### Particle size distribution

The pattern and distribution of aggregate ions/particles when they floc into discernible lumps are mostly displayed by the particle distribution plots. The cluster size distribution for colliding particles was obtained by deriving a generic expression, Eq. 2.9, from Eq. 2.8. This was done for particles of  $m$ th order, taking into account the fact that the coagulation–flocculation followed second-order kinetics and that the coagulation period is characterized by a twofold reduction in the total number concentration.

$$\frac{N_m(t)}{N_0} = \frac{\left[KN_0\left(\frac{t}{2}\right)\right]^{m-1}}{\left[1 + \left(KN_0\left(\frac{t}{2}\right)\right)\right]^{m+1}} \quad (2.8)$$

$$N_m(t) = 4N_0^m(Kt)^{m-1} \left[2 + (KN_0t)\right]^{-(m+1)} \quad (2.9)$$

where  $\sum N$  is the representation of the total number of particles. Applying derived Eq. 2.9 for  $m = 1, 2$ , and 3 allowed for the prediction of the time evolution of the aggregating particles, which are dimmers, trimmers, and monomers. Figure 8a–e is time evolution of the floc size distribution for studied coagulant dosages: (a) 0.2 g/L, (b) 0.4 g/L, (c) 0.6 g/L, (d) 0.8 g/L, (e) 1.0 g/L, while 8f is time evolution of the distribution of dimmers for studied coagulant dosages at pH 2. Closely inspection of Figs. 8a–e shows the trends of particle aggregation throughout time. A consistent pattern across all the figures indicates the particle dispersion predicted in a typical coagulation process. It can be seen from Figs. 8a–e that the number of large particles, or monomers, decreases more quickly than the total particle count, hence aiding the coagulation process. Dimmers and trimmers arise from the rapid destabilization of monomers. The coagulation process was aided by the fast destabilization of monomers, which led to the formation of dimmers and trimmers. These

**Fig. 5** SEM result of *Arto-*  
*carpus heterophyllus* **a** before  
coagulation–flocculation **b**  
sludge of dosage and pH at the  
constant time **c** sludge of dosage  
and time at constant pH

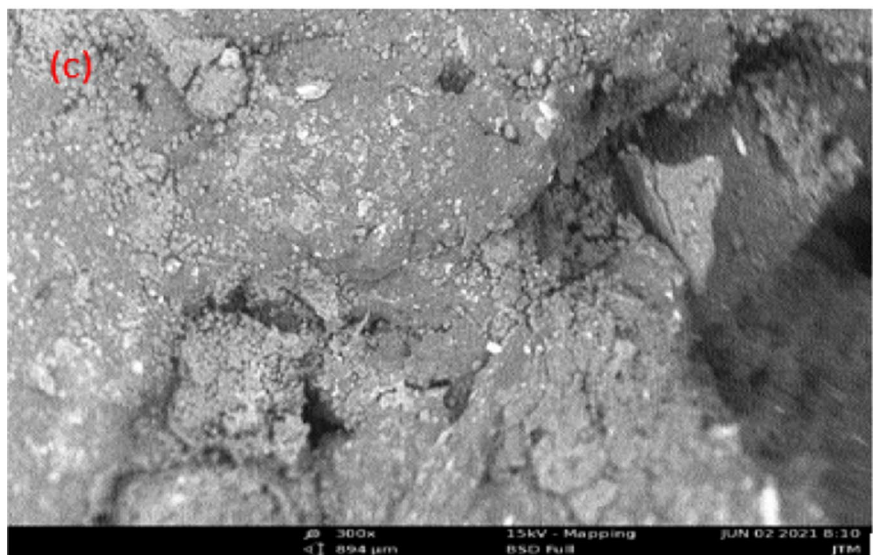
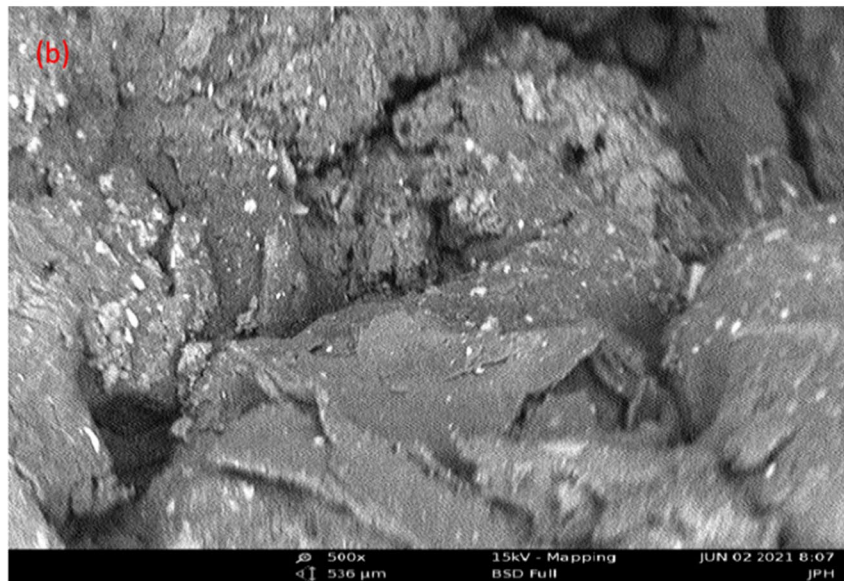
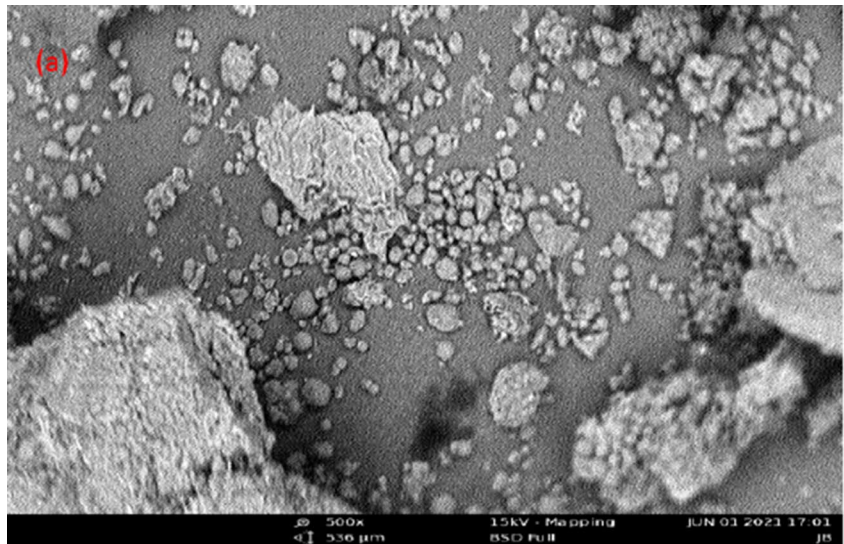


**Fig. 6** XRD diffractograms of (A) AH coagulant before the coagulation–flocculation process (B) AH sludge after the coagulation–flocculation process of coagulant dosage and pH at a constant time (C) AH sludge of coagulant dosage and time at constant pH

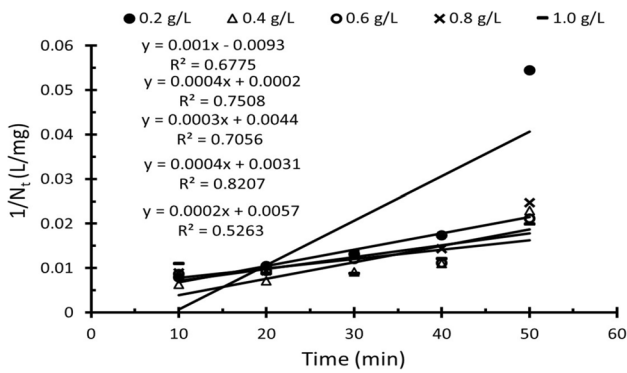
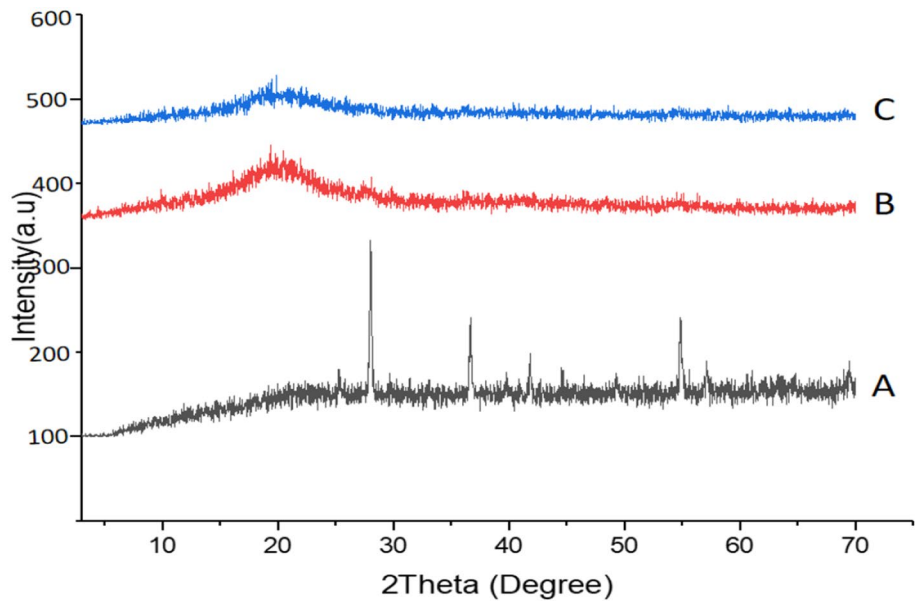


**Fig. 7** Kinetics plot of second-order reaction

highlight how well Eq. 2.9 fits the particle size distribution and aligns with earlier coagulation research (Nnaji et al. 2014; Ani et al. 2012). A dimmer trend is shown in Fig. 8f. It demonstrates that concentrations of larger floc sizes increase in the early stages of the coagulation process but fall in the later stages. An earlier work by Cao et al. (2011) supports this observation.

**Economic feasibility assessment**

The conventional activated sludge (CAS) technique allows the treatment of municipal wastewater via turbidity removal by assessing the reduction in total suspended solids (TSS). CAS systems, though they involve biological load reduction, have been applied to most wastewater treatment plants (WWTPs). It is estimated that in WWTPs with conventional activated sludge systems, aeration accounts for 50–60% of total electricity consumption and sludge treatment for 15–25% (Oulebsir et al. 2020). This inspired Nguyen et al. (2014) to work on aeration time optimization using the benchmark simulation model (BSM1) and the activated sludge model (ASM1). The results revealed a 30% increase in energy consumption for large WWTPs and a 70% gain for small WWTPs. It is therefore suggested that large WWTPs be installed for wastewater treatments to keep energy consumption to the barest minimum. The good thing is that biomass technologies are good alternatives for electricity generation and hence have a positive impact on energy demand in WWTPs (Oulebsir et al. 2020).

**Table 5** Functional coagulation–flocculation kinetics for different dosages and time at constant pH 2

Parameters	0.2 g/L	0.4 g/L	0.6 g/L	0.8 g/L	1.0 g/L
$R^2$	0.6775	0.7508	0.7056	0.8207	0.5263
$K$ (L g <sup>-1</sup> min <sup>-1</sup> )	0.0010	0.0004	0.0003	0.0004	0.0002
Rate equation (L g <sup>-1</sup> min <sup>-1</sup> )	0.0010	0.0004	0.0003	0.0004	0.0002
$\beta$ (L g <sup>-1</sup> min <sup>-1</sup> )	0.002	0.0008	0.0006	0.0008	0.0004
$K_R$ (L min <sup>-1</sup> )	1.5517E-20	3.880E-20	5.170E-20	3.880E-20	7.760E-20
$\epsilon$ (g <sup>-1</sup> )	6.4446E+16	1.030E+16	5.80E+15	1.030E+16	2.580E+15
$\tau_{1/2}$ (mins)	5.55556	13.8889	18.5185	13.8889	27.7778

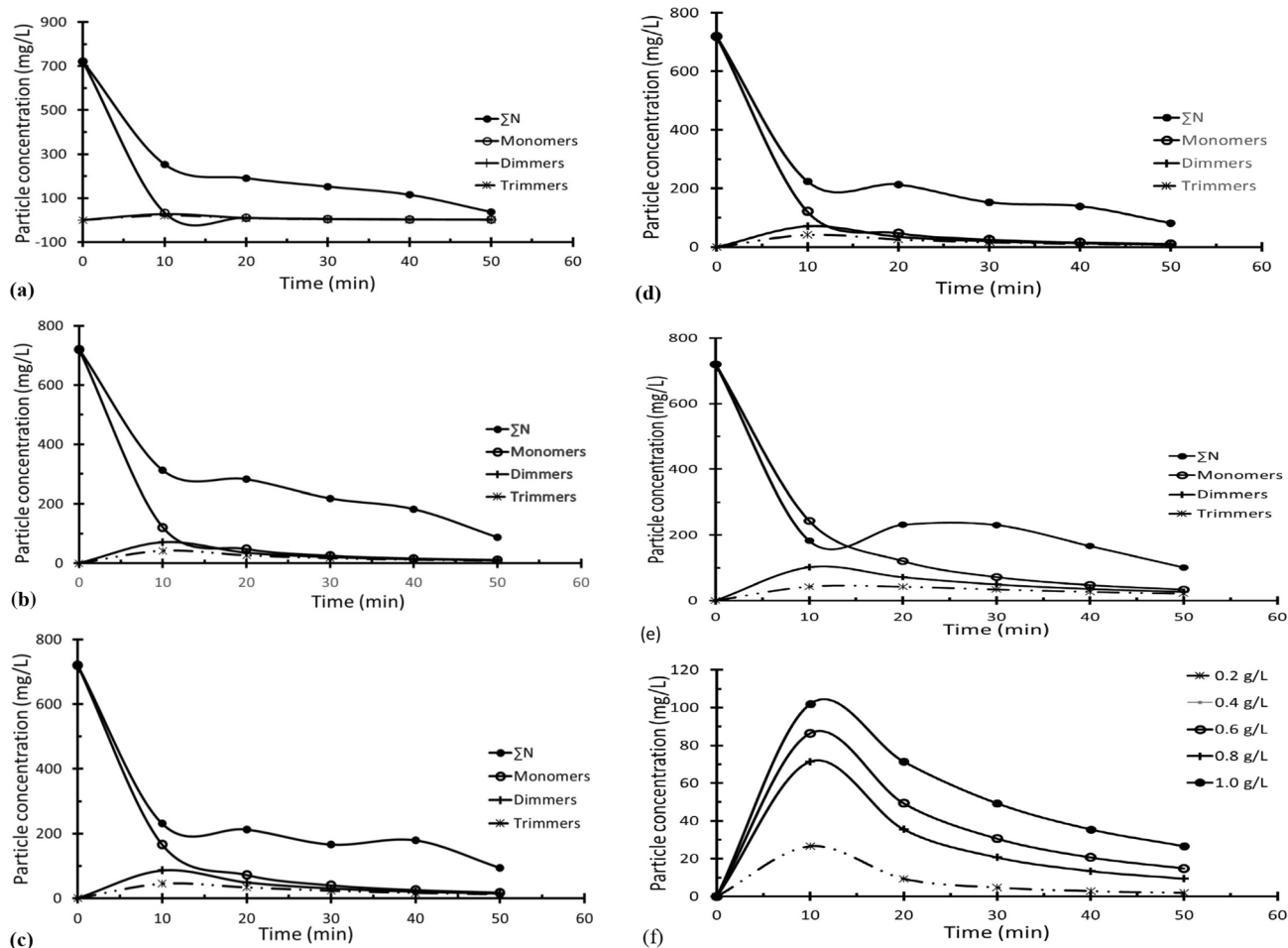


**Fig. 8** Time evolution of the flocculation process for studied coagulant dosages: **a** 0.2 g/L, **b** 0.4 g/L, **c** 0.6 g/L, **d** 0.8 g/L, **e** 1.0 g/L **f** time evolution of the distribution of dimmers for studied coagulant dosages, at pH 2

### Conclusion

AH coagulant is found to be an efficient natural coagulant in the treatment of paint effluent, for colour, turbidity, arsenic, mercury, and lead removal, under the optimal conditions of coagulant dosage of 0.2 g/L and pH 2, 0.8 g/L and pH 8, and 0.4 g/L and pH 10, all at a time of 50 min. FTIR spectra of the coagulant after the coagulation–flocculation process indicated some shifts in wave number indicating bond breakage and displacement of functional groups, hence the colour, turbidity, mercury, lead, arsenic, and other pollutants removal are suggested. The SEM image before the coagulation–flocculation process established that AH coagulant has a rough surface and tiny pores that aided the coagulation–flocculation process. The XRD pattern showed that the crystalline structure of the AH coagulant was altered to an amorphous structure after treatment. Coagulation–flocculation kinetics showed second-order kinetics fitting better. Also,  $\tau_{1/2}$  demonstrated a rapid coagulation–flocculation process of 0.6292 min.

**Supplementary Information** The online version contains supplementary material available at <https://doi.org/10.1007/s13201-024-02236-w>.

**Acknowledgements** The authors thank all the technologists of the Pure and Industrial Chemistry Department Unizik, Awka, for their resilience in this research.

**Author contributions** The conceptualization and design involved in this work were done by all the authors. Kelvin Obazie, Mmesoma Offorhze, Chiamaka Ifeaghalu, and Claudine I. Ogu prepared the materials and collected data, the data were analysed by Cecilia Aduaka and Ugomma C. Onyeije. Validation of the data by Ngozi A. Okonkwo, Nnaji Nnaemeka: data analysis and review writing. Ifeoma M. Iloamaeke supervised and wrote the first draft of the manuscript. All other authors provided feedback on earlier drafts. The final manuscript was read and approved by all writers.

**Funding** No funding was received.

### Declarations

**Conflict of interest** The authors have no competing interests to disclose.

**Ethical standards** All authors have approved the submission of this paper.

**Open Access** This article is licensed under a Creative Commons Attribution 4.0 International License, which permits use, sharing, adaptation, distribution and reproduction in any medium or format, as long as you give appropriate credit to the original author(s) and the source, provide a link to the Creative Commons licence, and indicate if changes were made. The images or other third party material in this article are included in the article's Creative Commons licence, unless indicated otherwise in a credit line to the material. If material is not included in the article's Creative Commons licence and your intended use is not permitted by statutory regulation or exceeds the permitted use, you will need to obtain permission directly from the copyright holder. To view a copy of this licence, visit <http://creativecommons.org/licenses/by/4.0/>.

## References

- Abdoulhassan MA, Souabi S, Yaacoubi A, Baudu M (2016) Coagulation efficacy of a tannin coagulant agent compared to metal salts for paint manufacturing wastewater treatment. *Desalin Water Treat*. <https://doi.org/10.1080/19443994.2015.1101016>
- Abdulsahib HT, Taobi AH, Hashim SS (2015) A novel coagulant based on lignin and tannin for bentonite removal from water. *IJAR* 3(2):426–442
- Abel JS, Stangle GC, Schilling CH, Aksay IA (1994) Sedimentation in flocculating colloidal suspensions. *J Mat Res* 9(2):451–461
- Ahmadi NC, Zanjanchi MA (2016) Use of *Descurainia Sophia L.* As a natural coagulant for the treatment of dye-containing wastewater. *Environ Prog Sustainable Energy* 35:996–1001
- Al-Shehri BM, Khder AERS, Ashour SS, Hamdy MS (2019) A review: the utilization of mesoporous materials in wastewater treatment. *Mater Res Express* 6(12):122002. <https://doi.org/10.1088/2053-1591/ab52af>
- Ani JU, Menkiti MC, Onukwuli OD (2010) Coagulation and flocculation behaviour of snail shell coagulant in fibre-cement plant effluent. *J Engr Appl Sci* 5:1–8
- Ani JU, Menkiti MC, Onukwuli OD (2011) Coagulation-flocculation performance of snail shell biomass for wastewater purification. *N Y Sci J* 4(2):81–90
- Ani JU, Nnaji NJN, Onukwuli OD, Okoye COB (2012) Nephelometric and functional parameters response of coagulation for the purification of industrial wastewater using *Detarium microcarpum*. *J Hazard Mat* 243:59–66
- Anu S, Anu N (2016) Feasibility of natural coagulant for the treatment of dairy wastewater. *Int J Sci Eng Res* 7(4):245–249
- AOAC (2000a) Oil in cereal adjuncts: petroleum ether extraction method. Official methods of analysis of AOAC international, method 94516, 17th edn. Assoc. of Official Analytical Chemists, Arlington, VA
- AOAC (1990a) Association of analytical chemistry, methods for proximate analysis. pp 2217–2280
- AOAC (2000b) Total, soluble, and insoluble dietary fiber in foods: enzymatic gravimetric method, MES-TRIS buffer. In: Official methods of analysis of AOAC international, method 991.43, 17th edn. Assoc. of Official Analytical Chemists, Arlington, VA
- AOAC (2005b) Determination of protein content in food, method 945.18-B. In: Official methods of analysis, AOAC International Publisher, Gaithersburg
- APHA 3112B (2012) Cold-vapour atomic absorption spectrophotometric method, standard methods for the examination of water and wastewater. 20th edn. American Public Health Association, Washington, D.C., USA
- APHA (1992) Standard methods for the examination of water and wastewater, in American public health association (APHA). In: American water works association (AWWA) and water pollution control federation (WPCF). 18th edn. Washington DC
- APHA (1995) Standard methods for the examination of water and wastewater, 19 edn. Washington, D.C., USA
- APHA (1998) Standard methods for the examination of water and wastewater, In: APHA, AWWA, and WEF, 20 edn
- Asantewah NM, Agyei EA, Opoku F (2021) Mineral and proximate composition of the meat and shell of three snail species. *Heliyon* 7:e08149. <https://doi.org/10.1016/j.heliyon.2021.e08149>
- Cao B, Gao B, Xu C, Fu Y, Liu X (2010) Effects of pH on coagulation behavior and floc properties in Yellow River water treatment using ferric based coagulants. *Chin Sci Bull* 55(14):1382–1387. <https://doi.org/10.1007/s11434-010-0087-5>
- Cao B, Gao B, Liu X, Wang M, Yang Z, Yue Q (2011) The impact of pH on floc structure characteristic of polyferric chloride in a low DOC and high alkalinity surface water treatment. *Water Res* 45(18):6181–6188
- Chen W, Zheng H, Teng H, Wang Y, Zhang Y, Zhao C, Liao Y (2015) Enhanced coagulation-flocculation performance of iron-based coagulants: effects of PO<sub>4</sub>(3-) and SiO<sub>3</sub>(2-) modifiers. *PLoSOne*. <https://doi.org/10.1371/journal.pone.0137116>
- Choy SY, Prasad KMN, Wu TY, Raghunandan ME, Yang B, Phang S-M, Ramanan RN (2016) Isolation, characterization and the potential use of starch from jackfruit seed wastes as a coagulant aid for treatment of turbid water. *Environ Sci Pollut Res* 24(3):2876–2889. <https://doi.org/10.1007/s11356-016-8024-z>
- Elango G, Elango S (2017) International journal of research in chemistry and environment physicochemical parameters of textile dyeing effluent and its impacts with case study. *Int J Res Chem Environ* 7(1):17–24
- El-Shazly MA, Hasanin EA, Kamel MM (2010) Appropriate technology for industrial wastewater treatment of paint industry. *Am Eurasian J Agric Environ Sci* 8(5):597–601
- EPA (1993) Method 180.1: determination of turbidity by nephelometry. Environmental monitoring systems laboratory office of research and development. U.S. Environmental protection agency, Cincinnati, Ohio, p 45268
- Fateatun N, Jiaur R, Sultan M, Sorifa A, Aminul IT, Maruf A (2014) Physicochemical properties of flour and extraction of starch from jackfruit seed. *Int J Nutr Food Sci*. 3(4):347–354. <https://doi.org/10.11648/j.ijnfs.20140304.27>
- FEPA (1999) Federal environmental protection agency act. Federal environmental protection agency, Lagos, Nigeria
- Gaikwad VT, Munavalli GR (2019) Turbidity removal by conventional and ballasted coagulation with natural coagulants. *Appl Water Sci* 9:130. <https://doi.org/10.1007/s13201-019-1009-6>
- Ghernaout D, Al-Ghonamy AI, Boucherit A, Ghernaout B, Naceur MW, Noureddine AM, Aichouni M, Mahjoubi AA, Elboughdiri NA (2015) Brownian motion and coagulation process. *Am J Environ Prot*. 4(1–5):1–15. <https://doi.org/10.11648/j.ajeps.2015040501.11>
- Ghughe SP, Saroha AK (2018) Catalytic ozonation for the treatment of synthetic and industrial effluents—application of mesoporous materials: a review. *J Environ Manag* 211:83–102. <https://doi.org/10.1016/j.jenvman.2018.01.052>
- Hubbe MA, Metts JR, Hermosilla D, Blanco MA, Yerushalmi L, Haghight F, Lindholm-Lehto P, Khodaparast Z, Kamali M, Elliott A (2016) Wastewater treatment and reclamation: a review of pulp and paper industry practices and opportunities. *BioRes* 11(3):7953–8091
- Iloamae IM, Julius CO (2019) Treatment of pharmaceutical effluent using seed of *Phoenix dactylifera* as a natural coagulant. *J Basic Phys Res* 9(1):91–100

- Iloamae IM, Egwuatu CI, Onwumelu HA, Nzoka-Okoye CE (2020) Optimization of colour reduction in the pharmaceutical effluent by response surface methodology. *Int J Environ Chem* 4(1):28–37. <https://doi.org/10.11648/j.ijec.20200401.14>
- Iloamae IM, Nnaji NJ, Okpala EC, Eboatu AN, Onuegbu TU (2021) *Mercenaria mercenaria* shell: coagulation-flocculation studies on colour removal by response surface methodology and nephelometric kinetics of an industrial effluent. *J Environ Chem Eng*. <https://doi.org/10.1016/j.jece.2021.105715>
- Islam MR, Mostafa MG (2020) Characterization of textile dyeing effluent and its treatment using polyaluminum chloride. *Appl Water Sci*. <https://doi.org/10.1007/s13201-020-01204-4>
- Jabar JM, Yisau AO, Kazeem AA, Ahmed IB (2020) Kinetics and mechanisms of congo-red dye removal from aqueous solution using activated *Moringa oleifera* seed coat as adsorbent. *Appl Water Sci* 10:136. <https://doi.org/10.1007/s13201-020-01221-3>
- Jachimowicz P, Cydzik-Kwiatkowska A (2022) Coagulation and flocculation before primary clarification as efficient solutions for low-density microplastic removal from wastewater. *Int J Environ Res Public Health* 19:13013. <https://doi.org/10.3390/ijerph192013013>
- Jatto OE, Asia IO, Medjor WE (2010) Proximate and mineral composition of different species of snail shell. *Pac J Sci Technol* 11(1):416–419
- Lasaki BA, Maurer P, Schonberger H (2023) Effect of coupling primary sedimentation tank (PST) and microscreen (MS) to remove particulate organic carbon (POC): a study to mitigate energy demand in municipal wastewater treatment plants. *Sustain Environ Res* 33:25. <https://doi.org/10.1186/s42834-023-00186-7>
- Lasaki BA, Maurer P, Schonberger H, Alvarez EM (2023) Empowering municipal wastewater treatment: enhancing particulate organic carbon removal via chemical advanced primary treatment. *Environ Technol Innov*. <https://doi.org/10.1016/j.eti.2023.103436>
- Liu J, Cheng S, Cao N, Geng C, He C, Shi Q, Zhao H (2018) Actinia-like multifunctional nanocoagulant for single-step removal of water contaminants. *Nat Nanotechnol*. <https://doi.org/10.1038/s41565-018-0307-8>
- Madukasi EI, Ajuebor FN, Ojo B, Meadows AB (2009) Pollution removal from paint effluents using modified clay minerals. *J Ind Res Technol* 2(1):49–55
- Malakootian M, Almasi A, Hossaini H (2008) Pb and Co removal from paint industries effluent using wood ash. *Int J Environ Sci Tech* 5(2):217–222
- Marzougui Z, Damak M, Elleuch B, Elaissari A (2018) Occurrence and enhanced removal of heavy metals in industrial wastewater treatment plant using coagulation-flocculation process. *Adv Sci, Technol Innov*. [https://doi.org/10.1007/978-3-319-70548-4\\_163](https://doi.org/10.1007/978-3-319-70548-4_163)
- Menkiti MC, Onukwuli OD (2011) Coag-Flocculation studies of *Azelia belia* coagulant (ABC) in coal effluent using single and stimulated multiangle nephelometry. *J Miner Mater Charact Eng* 10(3):279–298
- Menkiti MC, Aneke MC, Ejikeme PM, Onukwuli OD (2014) Adsorptive treatment of brewery effluent using activated cheysophyllum albidium seed shell. *Springer Plus* 3:213
- Menkiti MC, Ezemagu IG, Nwoye CI, Ejimofor MI (2015a) Post-treatment sludge analyses and purification of paint effluent by coag-flocculation method. *Int J Energy Environ Eng* 2016(7):69–83. <https://doi.org/10.1007/s40095-015-0192-y>
- Menkiti MC, Ejimofor MI (2016) Experimental and artificial neural network application on the optimization of paint effluent (PE) coagulation using novel Achatinoidea shell extract (ASE). *J Water Process Eng* 10:172–187. <https://doi.org/10.1016/j.jwpe.2015.09.01>
- Menkiti MC, Ezemagu IG, Nwoye CI, Ejimofor MI (2015b) Post-treatment sludge analyses and purification of paint effluent by coag-flocculation method. *Int J Energy Environ Eng* 7:69–83. <https://doi.org/10.1007/s40095-015-0192-y>
- Menkiti MC, Okoani AO, Ejimofor MI (2018) Adsorptive study of coagulation treatment of paint wastewater using novel *Brachystegia eurycoma* extract. *Applied Water Science*. 8:189. <https://doi.org/10.1007/s13201-018-0836-1>
- Mohamad Sy SF, Mohd Said F, Abdul Munaim MS, Mohamad S, Wan Sulaiman WMA (2019) Proximate composition, minerals contents, functional properties of Mastura variety jackfruit (*Artocarpus heterophyllus*) seeds and lethal effects of its crude extract on zebrafish (*Danio rerio*) embryos. *Food Res* 3(5):546–555
- Mohammed SJ, Husain IAF, Kabashi NA, Abdullah N (2012) Multiple inputs artificial neural network model for the prediction of wastewater treatment plant performance. *Aust J Basic Appl Sci* 6(1):62–69
- Mohan D, Pittman CU (2007) Arsenic removal from water/ wastewater using adsorbents: a critical review. *J Hazard Mater* 142(1):1–53. <https://doi.org/10.1016/j.jhazmat.2007.01.006>
- Mohanad JA, Radin M, Al-Sahari M, Al-Gheethi A, Daud AMM (2021) Optimizing FeCl<sub>3</sub> in coagulation-flocculation treatment of dye wastes. *Songklanakarin J Sci Technol* 43(4):1094–1102
- Naim R, Pei Sean G, Nasir Z, Mokhtar NM, Safiah Muhammad NA (2021) Recent Progress and challenges in hollow fiber membranes for wastewater treatment and resource recovery. *Membranes* 11:839. <https://doi.org/10.3390/membranes11110839>
- Namasivayam C, Kadirvelu K (1999) Uptake of mercury (II) from wastewater by activated carbon from an unwanted agricultural solid by-product: coirpith. *Carbon* 37(1):79–84. [https://doi.org/10.1016/S0008-6223\(98\)00189-4](https://doi.org/10.1016/S0008-6223(98)00189-4)
- Naseem R, Tahir SS (2001) Removal of Pb (II) from aqueous/acidic solutions by using bentonite as an adsorbent. *Water Res* 35(16):3982–3986
- Natumanya R, Okot-Okumu J (2015) Evaluating coagulant activity of locally available *syzygium cumini*, *Artocarpus heterophyllus* and *Moringa oleifera* for treatment of community drinking water, Uganda. *Int J Biol Chem Sci* 9(6):2535–2554
- Ngadi N, Yusoff NA (2013) Treatment of textile wastewater using biodegradable flocculants of chitosan and extracted pandan leaves. *Jurnal Teknologi*. <https://doi.org/10.11113/jt.v64.1647>
- Nguyen DH, Dagot C, Roche N (2014) Optimisation de la conception et du fonctionnement des stations de traitement des eaux usées. PhD thesis, Université de Lorraine
- Nnaji NJN, Ani JU, Aneke LE, Onukwuli OD, Okoro UC, Ume JI (2014) Modelling the coag-flocculation kinetics of cashew nut testa tannins in an industrial effluent. *J Ind Chem* 20:1930–1935
- Okolo BI, Nnaji PC, Menkiti MC, Onukwuli OD (2015) A kinetic investigation of the pulverized okra pod induced coag-flocculation in treatment of paint wastewater. *Am J Anal Chem* 6:610–622
- Okuda T, Baes AU, Nishijima W, Okada M (1999) Improvement of extraction method of coagulation active components from *Moringa oleifera* seed. *Water Res* 33(15):3373–3378
- Oulebsir R, Lefkir A, Safri A, Bermad A (2020) Optimization of the energy consumption in activated sludge process using deep learning selective modeling. *Biomass Bioenerg* 132:105420
- Pang FM, Kumar P, Teng TT, Mohd Omar AK, Wasewar KL (2011) Removal of lead, zinc and iron by coagulation–flocculation. *J Taiwan Inst Chem Eng* 42(5):809–815. <https://doi.org/10.1016/j.jtice.2011.01.009>
- Pena ME, Korfiatis GP, Patel M, Lippincott L, Meng X (2005) Adsorption of As (V) and As(III) by nanocrystalline titanium dioxide. *Water Res* 39(2005):2327–2337
- Raychaudhuri SS, Paulami P, Talukder P, Basak A (2021) Polyamines, metallothioneins, and phytochelatins: Natural defense of plants to mitigate heavy metals. *Stud Nat Prod Chem* 69:227–261. <https://doi.org/10.1016/B978-0-12-819487-4.00006-9>
- Sakhi D, Rakhila Y, Elmchauri A, Abouri M, Souabi S, Jada A (2019) Optimization of coagulation flocculation process for the removal of heavy metals from real textile wastewater. In: Ezziyyani M

- (ed) Advanced intelligent systems for sustainable development (AI2SD'2018). Advances in intelligent systems and computing. Springer, Cham. [https://doi.org/10.1007/978-3-030-11881-5\\_22](https://doi.org/10.1007/978-3-030-11881-5_22)
- Sivaranjini LU, Abarajitha K (2020) Proximate analysis of jack fruit seed flour (Non-germinated and germinated) and value addition to bread. *Int J Appl Res* 6(5):293–299
- Sreeletha A, Lini J, Dhanyalekshmi CS, Sabu KR, Chandran P (2017) Phytochemical, proximate, antimicrobial, antioxidant and FTIR analysis of seeds of *Artocarpusheterophyllus* Lam. *Adv Biotechnol Microbiol* 5(1):16–24. <https://doi.org/10.19080/AIBM.2017.05.5556530019>
- Suffian Yusoff M, Zuki NAM, Zamri MFMA (2016) Effectiveness of jackfruit seed starch as coagulant aid in landfill leachate treatment process. *Int J GEOMATE* 11(26):2684–2687
- Sultana A, Amin MN, Miah MY, Sarker AK, Mahabub AR, Aziz MT, Sharmin F, Abdul H, Shiddika H, Emon SH, Tuli TP, Monira K (2017) Determination of proximate composition and amino acid profile of jackfruit seed and utilization of its seed flour for development of protein enriched supplementary food. *Cell Biol* 5(6):57–65. <https://doi.org/10.11648/j.cb.20170506.11>
- Suzihaque MUH, Md Zaki NA, Alwi H, Umami KI, Karim SFA, Anuar NK (2022) Jackfruit seed as an alternative replacement for starch flour. *Mater Today: Proc* 63(1):S451–S455. <https://doi.org/10.1016/j.matpr.2022.04.117>
- Teh CY, Wu TY, Juan JC (2014) Optimization of agro-industrial wastewater treatment using unmodified rice starch as a natural coagulant. *J Ind Crops Prod* 56:17–26. <https://doi.org/10.1016/j.indcrop.2014.02.018>
- Thamer JM, Shakir E (2017) Effect of settling time, velocity gradient, and camp number on turbidity removal for oilfield produced water. *Egypt J Pet* 27(1):31–36. <https://doi.org/10.1016/j.ejpe.2016.12.006>
- Vajihinejad V, Gumfekar SP, Bazoubandi B, Najafabadi ZR, Soares JBP (2019) Water soluble polymer flocculants: synthesis, characterization, and performance assessment. *Macromol Mater Eng* 304:1800526. <https://doi.org/10.1002/mame.20180052>
- Vishali S, Agrawal A (2017) Performance evaluation of polysaccharides eluted from *Cyamopsis tetragonolobus* (guar gum), as a natural coagulant, in the treatment of paint industry effluent. *Desalin Water Treat* 62:443–448. <https://doi.org/10.5004/dwt.2017.20130>
- Vishali S, Karthikeyan R (2018) Application of green coagulants on paint industry effluent- a coagulation-flocculation kinetic study. *Desalin Water Treat* 122:112–123. <https://doi.org/10.5004/dwt.2018.22703>
- WHO (World Health Organization) (2006) A compendium of standards for wastewater reuse in the Eastern Mediterranean
- Yadav A, Sahu PK, Patel KS, Lata L, Milosh H, Corns WT, Martín-Ramos P (2020) Assessment of arsenic and heavy metal pollution in Chhattisgarh, India. *J Hazard, Toxic, Radioact Waste* 24(1):05019008. [https://doi.org/10.1061/\(asce\)hz.2153-5515.0000478](https://doi.org/10.1061/(asce)hz.2153-5515.0000478)

**Publisher's Note** Springer Nature remains neutral with regard to jurisdictional claims in published maps and institutional affiliations.